BURNING UNCONTAINED OIL SLICKS: LARGE SCALE TESTS AND MODELLING

I.A. Buist
S.L. Ross Environmental Research Limited
Ottawa, Ontario
and
E.M. Twardus
Energetex Engineering
Waterloo, Ontario

INTRODUCTION

This paper describes the completion of the work reported previously (Buist and Twardus, 1984) on the ignition and burning of uncontained, batch oil spills in open water.

The premise of the study was based on the idea that, if a large, thick slick of oil is ignited, and the flames spread to cover the majority of the slick before it thins to less than one millimetre, very high oil removal efficiencies are possible. As the fire grows it can be postulated that the air entrained by the combustion and the thermal plume reduce the spreading rate of the oil and, at some critical fire size, stop the spreading, resulting in potentially very high oil combustion efficiencies.

The project was funded by Environment Canada, through the Arctic Marine Transportation Program, and the United States Coast Guard. Sohio Alaska Petroleum Company provided funds and logistics to support the large-scale testing in Prudhoe Bay Alaska. This paper covers the results of these tests and the results of the modelling of uncontained combustion.

OBJECTIVES

The objective of large scale tests was to measure the spreading rates of oil and flame, combustion efficiencies and self-induced wind herding with oil slicks which were an order-of-magnitude larger than those in the previous work. The objective of the modelling was to develop expressions to predict the phenomena observed as a result of the tests and estimate permissible ignition delays, combustion efficiencies and the number of igniters required for spills in the 10^2 to 10^4 m^3 size range.

LARGE SCALE TESTS

Methods

These tests were conducted in a 45 m x 67 m shallow test pit near Sohio Alaska Petroleum Company's East Dock facility in Prudhoe Bay, Alaska. The minimum water depth was 15 cm. At the centre of the pit (see Figure 1 and Plate 1) a 30 cm high, 6 m diameter sheet metal ring was balanced on four stakes and held in a circular shape by several stakes placed inside the ring around its circumference.

Environment Canada. Arctic and Marine Oilspill Program (AMOP) Technical Seminar, 8th. Proceedings. June 18-20, 1985, Edmonton, Alberta, Canada, Environment Canada, Ottawa, Ontario, 103-130 pp, 1985.

FIGURE 1 TEST PIT LAYOUT - PLAN VIEW

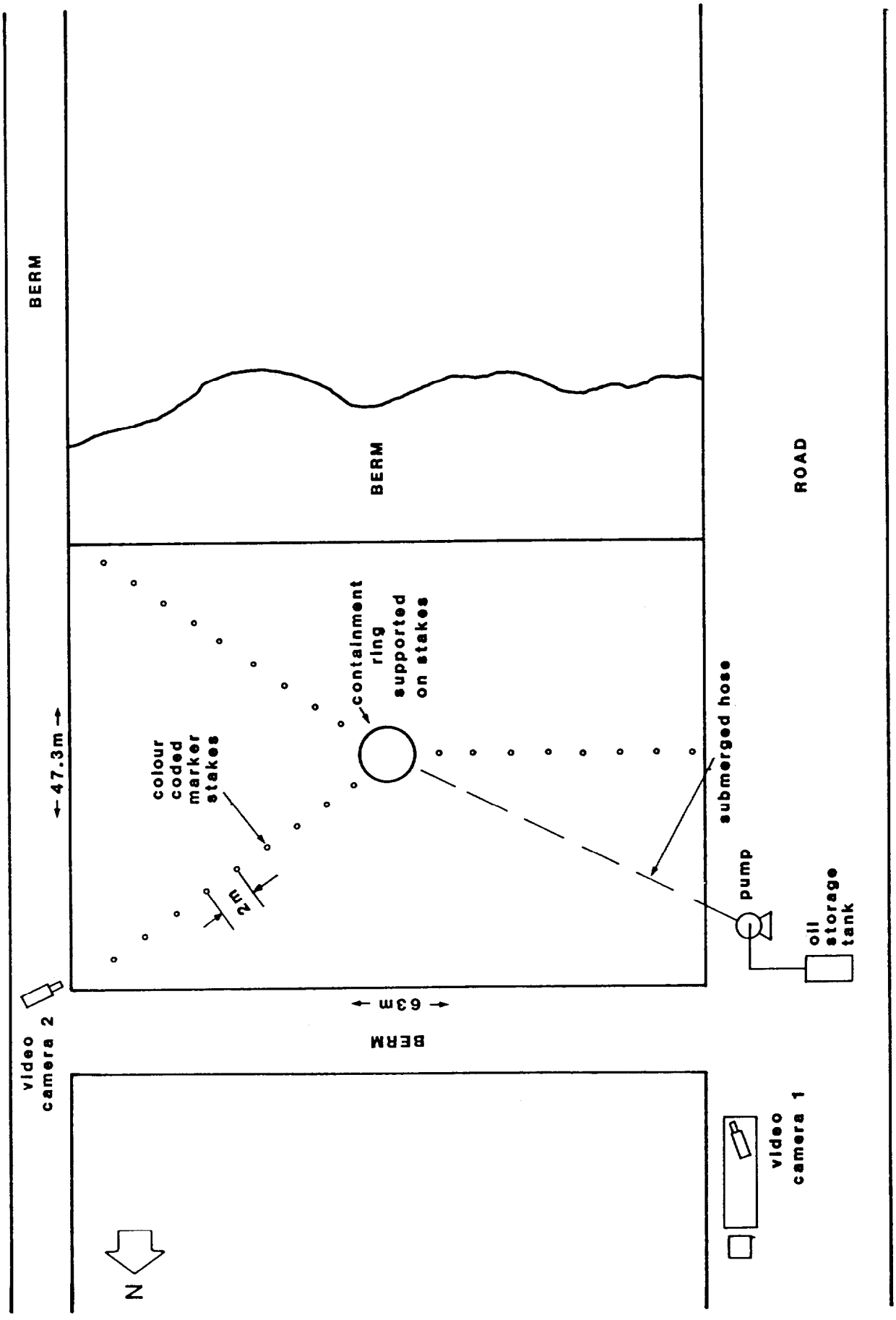

PLATE 1 - VIEW OF TEST PIT FROM SOUTH-WEST CORNER

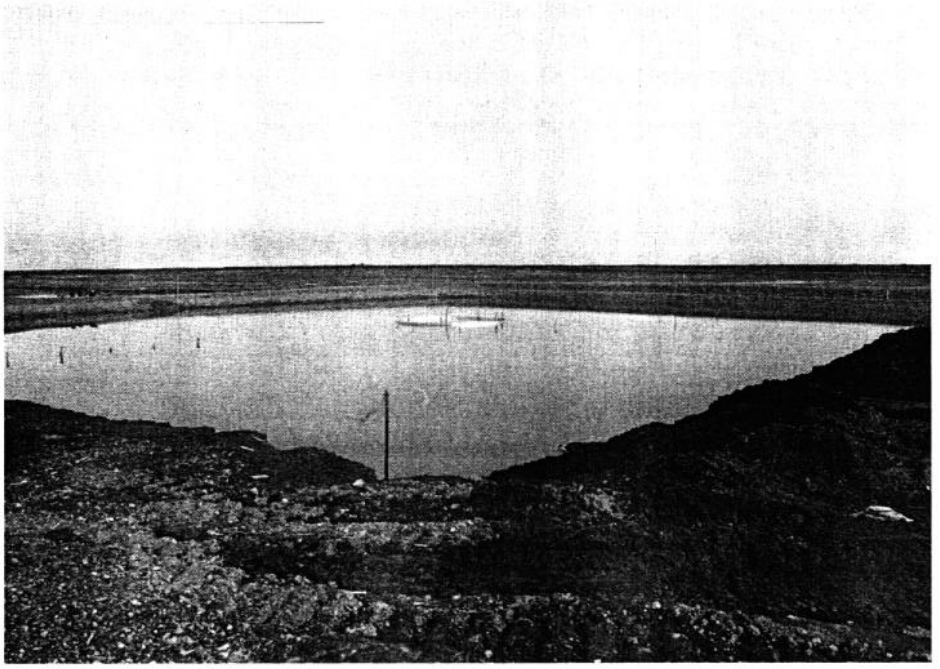

PLATE 2 - PUMPING OIL INTO RING (FROM NORTH-WEST CORNER)

Stakes were also driven into the pit bottom, at 2 m intervals out from the geometric centre of the ring, to aid in visually estimating the size of the oil slick. Each stake was colour-coded wth surveyor's tape.

Prior to each test a specified volume of Prudhoe Bay Crude oil (measured by dipping the storage tank) was pumped into the ring through a submerged hose (Plate 2). The properties of the crude oils used for each test are given in Table 1. Gas chromatographs and further data may be found in the report. Tests 1 and 2 were designed to measure oil and flame spreading and combustion efficiency for instantaneously ignited slicks. Test 3 was designed to measure combustion rate and air entrainment, and test 4 was designed to evaluate the effect of delayed ignition.

For test 1, 2 and 3 the oil inside the ring was ignited using a propane weed burner (Plate 3). In tests 1 and 2 once the flames had spread (Plate 4) the ring was dropped (Plate 5) by pulling out the supporting stakes using ropes from the sides of the pit. Each burn was recorded on videotape (see Figure 1 for placement) to document oil and flame spreading.

TABLE 1

PROPERTIES OF PRUDHOE BAY CRUDES

PROPERTY	OIL FOR TEST NUMBER:		
	1	2 and 3	4
DENSITY @ 15°C (g/cm^3)	0.8951	0.8934	0.8956
VISCOSITY @ 15°C (cSt)	38	46	45
INTERFACIAL TENSION @ 15°C (dynes/cm)			
OIL/AIR	26.8	26.6	25.7
OIL/WATER	23.4	23.4	24.3
WATER/AIR	62.1	65	65.6
FLASH POINT (°C - OPEN CUP)	20	1	11
FIRE POINT (°C - OPEN CUP)	74	60	63

PLATE 3 - IGNITING OIL IN RING

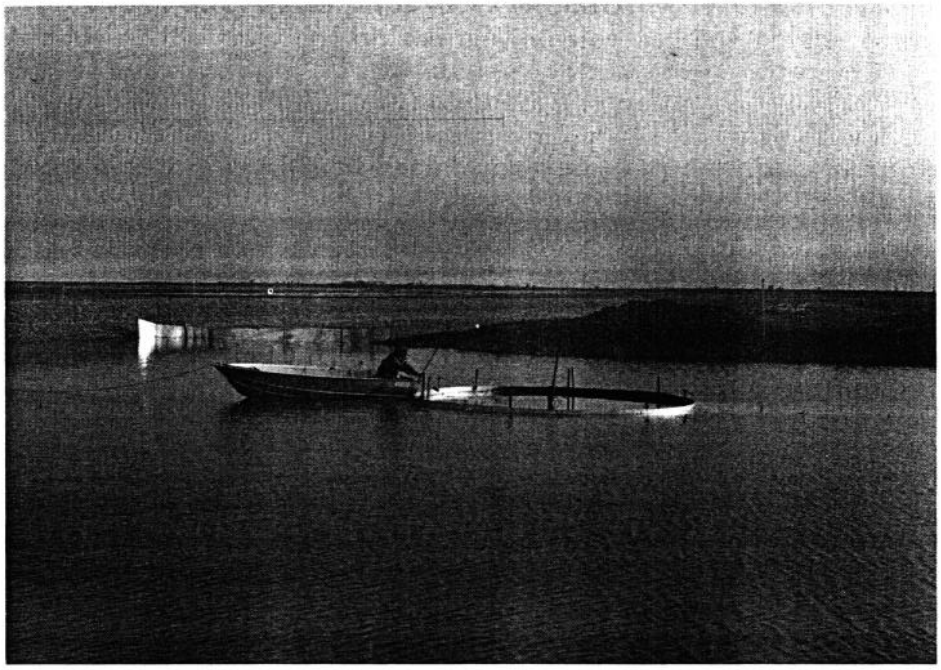

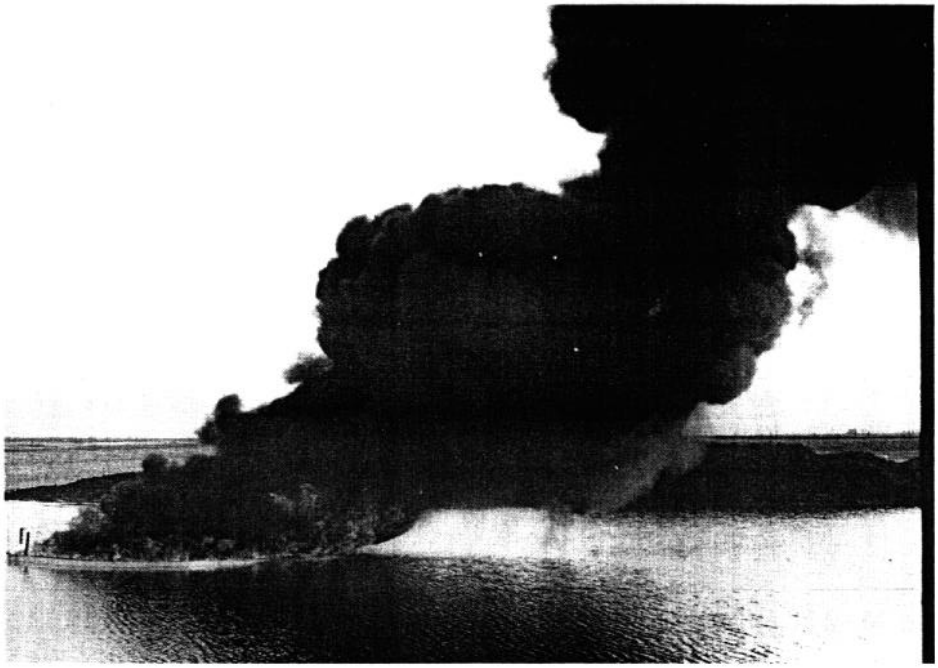

PLATE 4 - OIL SURFACE COMPLETELY ON FIRE

PLATE 5 - RING DROPPED

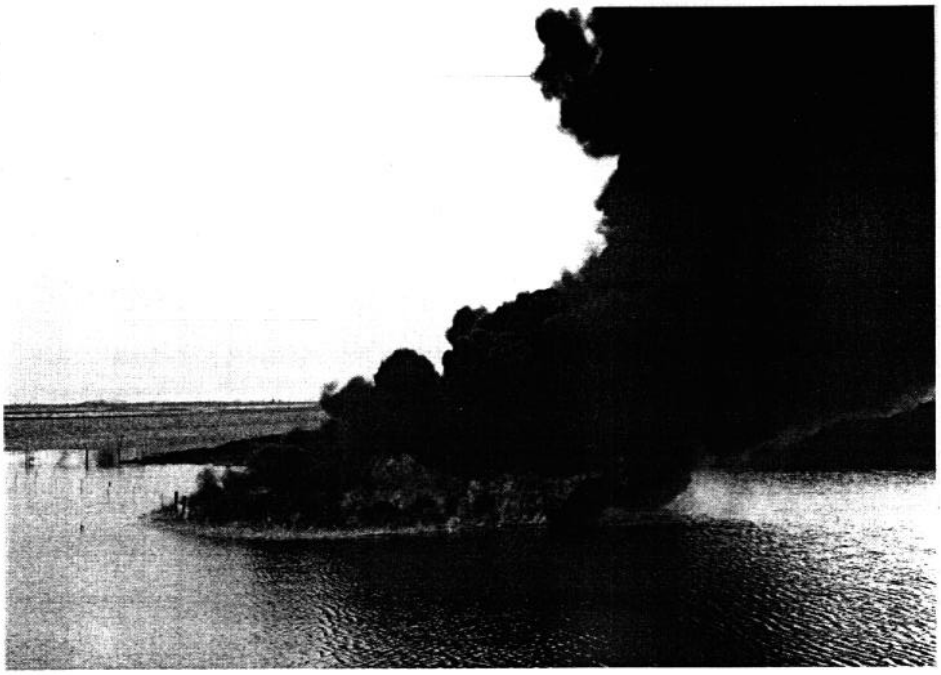

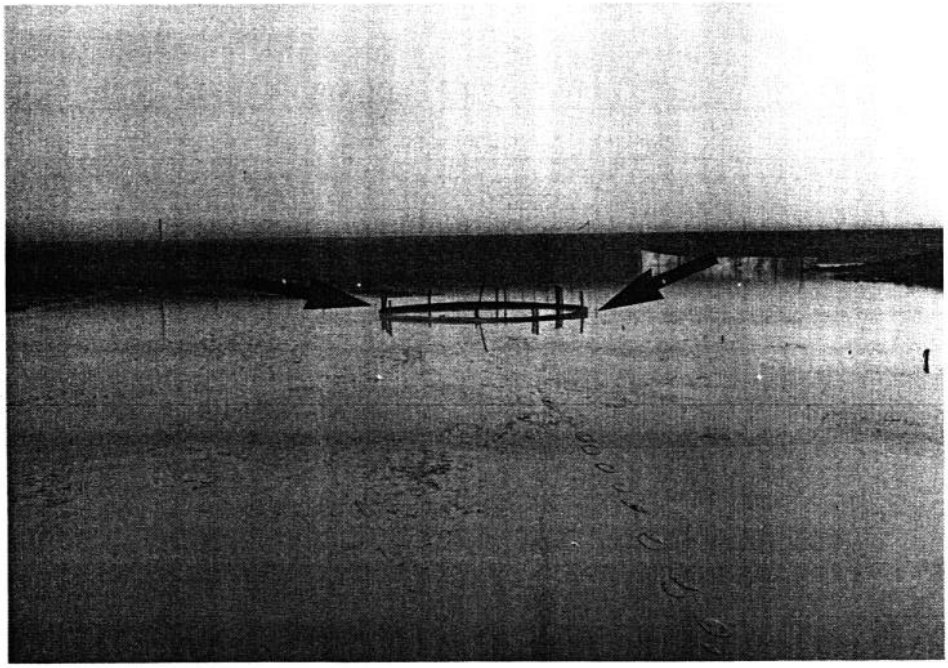

PLATE 6 - PITOT TUBE PLACEMENT FOR TEST 3
(ARROWS SHOW LOCATION)

For test 3 two bi-directional pitot tubes (McCaffrey, 1976) were placed about 15 cm from the outside of the ring, one on the upwind side and one on the downwind side to measure entrained air velocities (Plate 6). These were connected to individual electronic manometers and strip chart recorders (Plate 7).

The burning oil was contained within the ring for the duration of test 3.

For test 4, eight baking trays, each supported on two stakes, were placed about 1 cm above the water, approximately 1 m from the outer edge of the ring, spaced evenly around the ring's circumference (about 3 m apart). An oil soaked sorbent pad was placed in each tray, the tray was filled with oil and ignited (Plate 8). Once all the trays were burning vigourously the ring was dropped and the oil released (Plate 9).

After each test the oil residue was collected and weighed. After test 1 sorbents were used (Plate 10) but after tests 2, 3 and 4 the residue was concentrated using shovels, picked up off the water and placed in buckets and garbage bags.

After the tests were completed, the videotapes were analysed to determine oil and flame widths from the two cameras at right angles. It was assumed that each slick was elliptical in shape, thus its area as a function of time could be calculated from:

$$A = \pi ab \qquad (1)$$

where A = area of slick (m^2)
a = width of slick from camera 1 (m)
b = width of slick from camera 2 (m)

PLATE 7 - ELECTRONIC MANOMETERS AND CHART RECORDERS

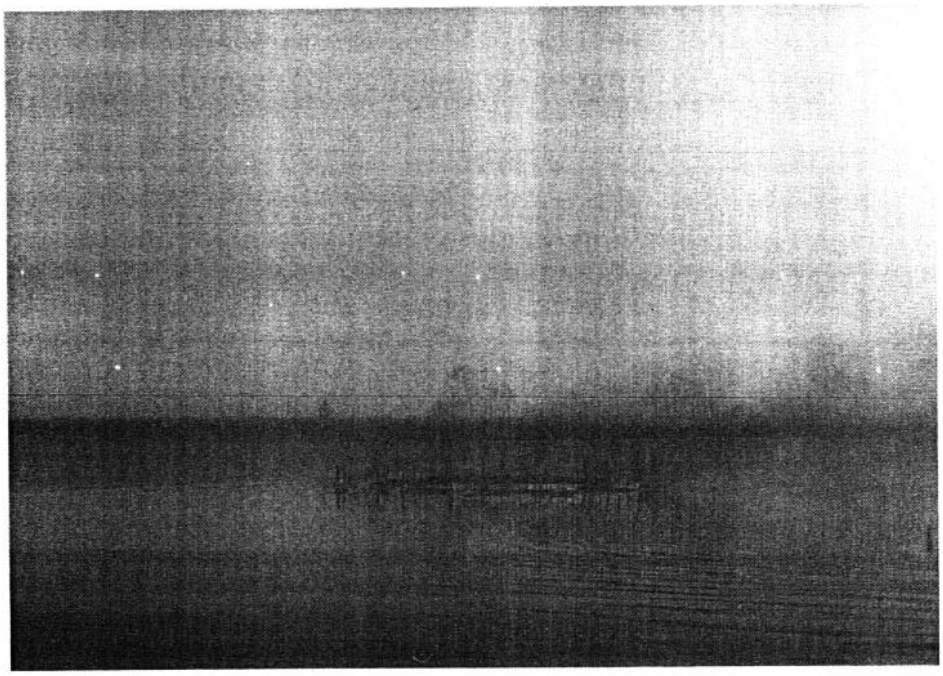

PLATE 8 - PLACEMENT OF BURNING OIL TRAYS FOR TEST

PLATE 9 - DROPPING RING, TEST 4

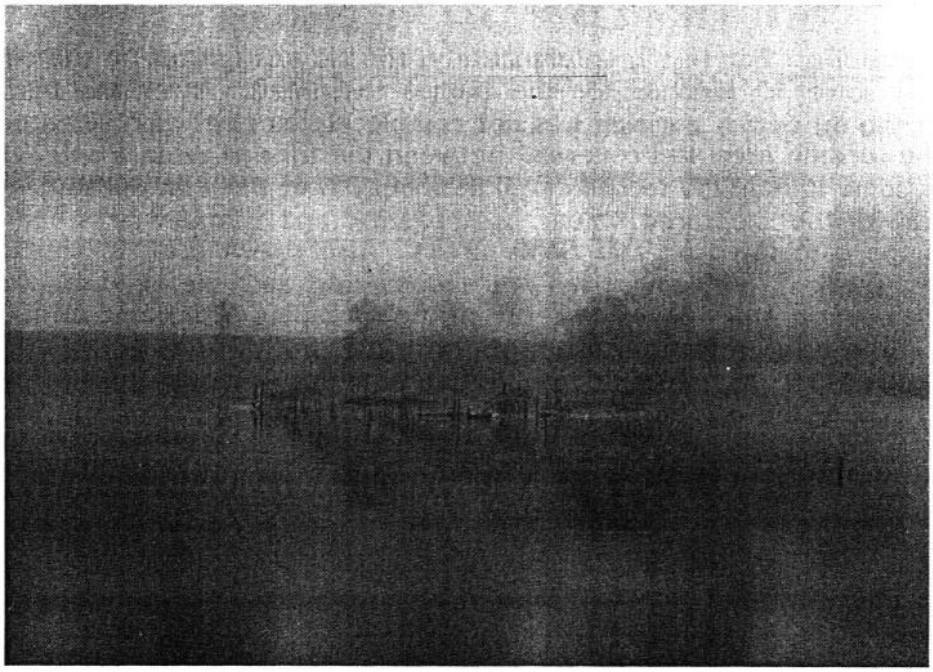

PLATE 10 - RESIDUE RECOVERY, TEST 1

Results and Discussion

Table 2 summarizes the conditions and results of each of the tests.

Oil and Flame Spreading. For test 1, unfortunately, the oil was ignited on the downwind edge and it took some 90 seconds for the flames to spread. After the test it was determined that the oil within the ring was not completely on fire when released. Only about 75% of the surface area was covered. Between the time of release and extinction the slick drifted some 10 m in 150 sec (10 cm/s) at about 3% of the wind speed.

Figure 2 shows the measured values of the slick and flame widths for Test 1. Figure 3 shows the calculated oil and flame areas. Also shown are the predicted oil slick area (Fay, 1969) if no combustion were occurring and the predicted area of combustion using equations developed to describe the spreading of burning oil (S.L. Ross and Energetex, 1985).

The difference between actual and predicted slick spreading may be because the inflow of air to supply the combustion slowed the oil spreading. The predicted flame area differs from the actual because the model is based on instantaneous ignition of the entire slick area. In test 1 only 75% of the slick was on fire when it was released.

Figure 4 shows the slick and flame widths calculated for test 2 (same procedure as test 1 with 30% more oil). Figure 5 shows the predicted and calculated oil and flame areas as a function of time. In this case Fay's model only slightly overestimates the intitial oil spreading; however, it can be seen that once the flames reached an area of about 300 m^2 the oil spreading was retarded for some 30 seconds, likely due to the effects of the induced flow of air into the fire. The predicted flame area does agree fairly well with the observed flame area. The predicted combustion efficiency of 92% agrees well with the results. Figure 6 shows the measured flame widths for test 4 (the oil slick could not be distinguished from the water because of the foggy, flat calm conditions) in which the oil was released then ignited around its periphery by a circle of burning pans. Figure 7 compares the calculated flame area with that predicted by the burning model and Fay's oil spreading model. Taking into account the delay in ignition the predicted and actual flame spreading are quite close. The predicted combustion efficiency of 91% agrees well with the measured value at 88.3%.

TABLE 2

RESULTS OF LARGE SCALE TEST BURNS

	TEST NO. 1	2	3	4
Initial Oil Volume (l)	958	1343	575	1273
Initial Oil Weight (kg)	857	1200	342	1140
Initial Oil Thickness (mm)	33	47	20	40
Ignition & Release	ignited & released	ignited & released	ingited, not released	released then ignited
Wind Speed (m/s)	2	2.5	0-2	2.5
Air Temperature (°C)	-1	2	0	1
Water Temperature (°C)	0	0	0	0
Residue Oil Volume (l)	N.M.*	120	N.M.	N.M.
Residue Oil Weight (kg)	240	109	62	133
Combustion Efficiency (wt.%)				
TOTAL	72	90.9	87.9	88.3
CORRECTED+	70.9	90.6	---	---

* N.M. - not measured

\+ initial oil volume reduced by amount burnt prior to dropping ring.

FIGURE 2 OIL AND FLAME WIDTH - TEST 1

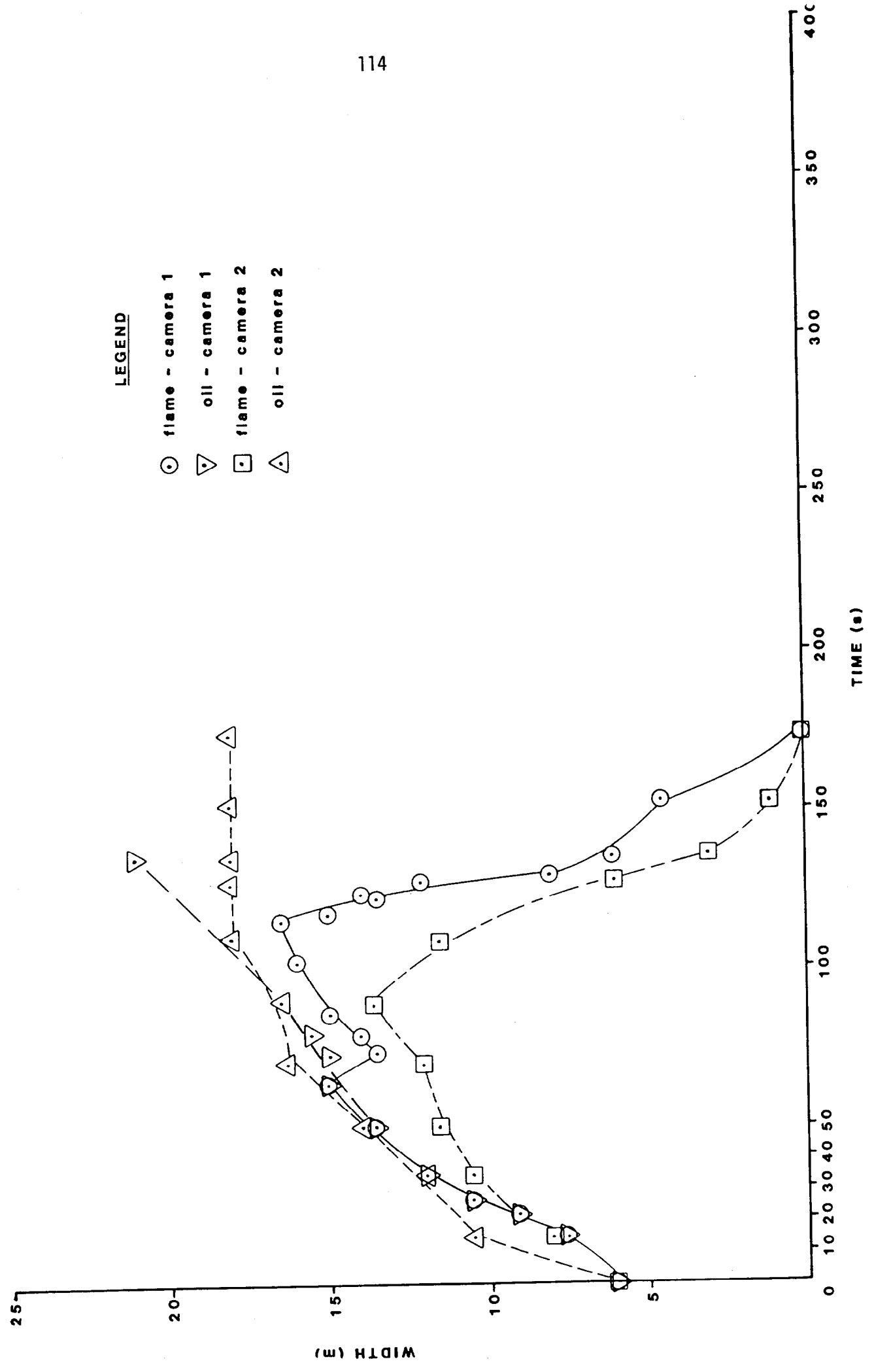

FIGURE 3 CALCULATED OIL AND FLAME AREA - RUN 1

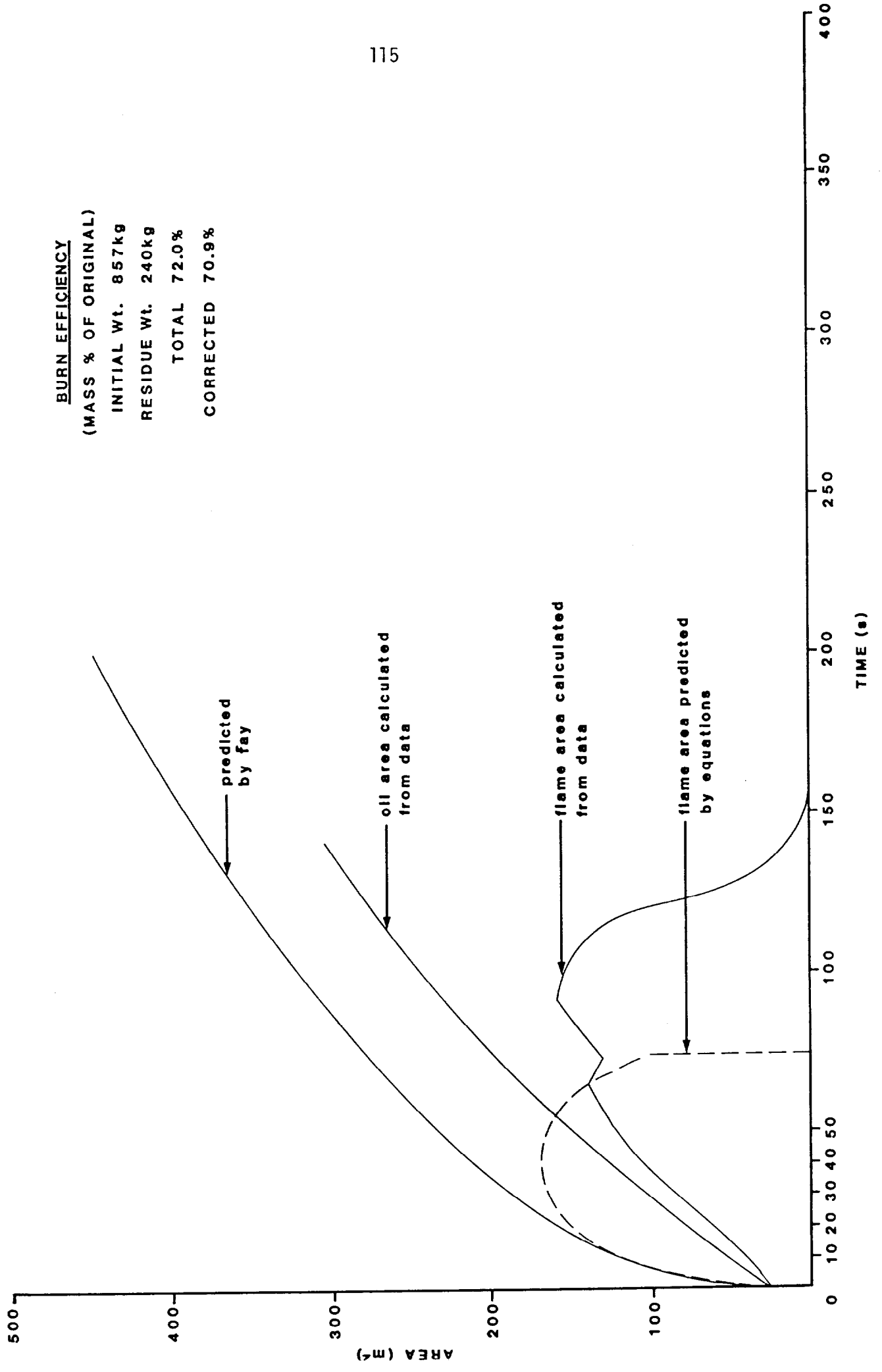

FIGURE 4 OIL AND FLAME WIDTH - RUN 2

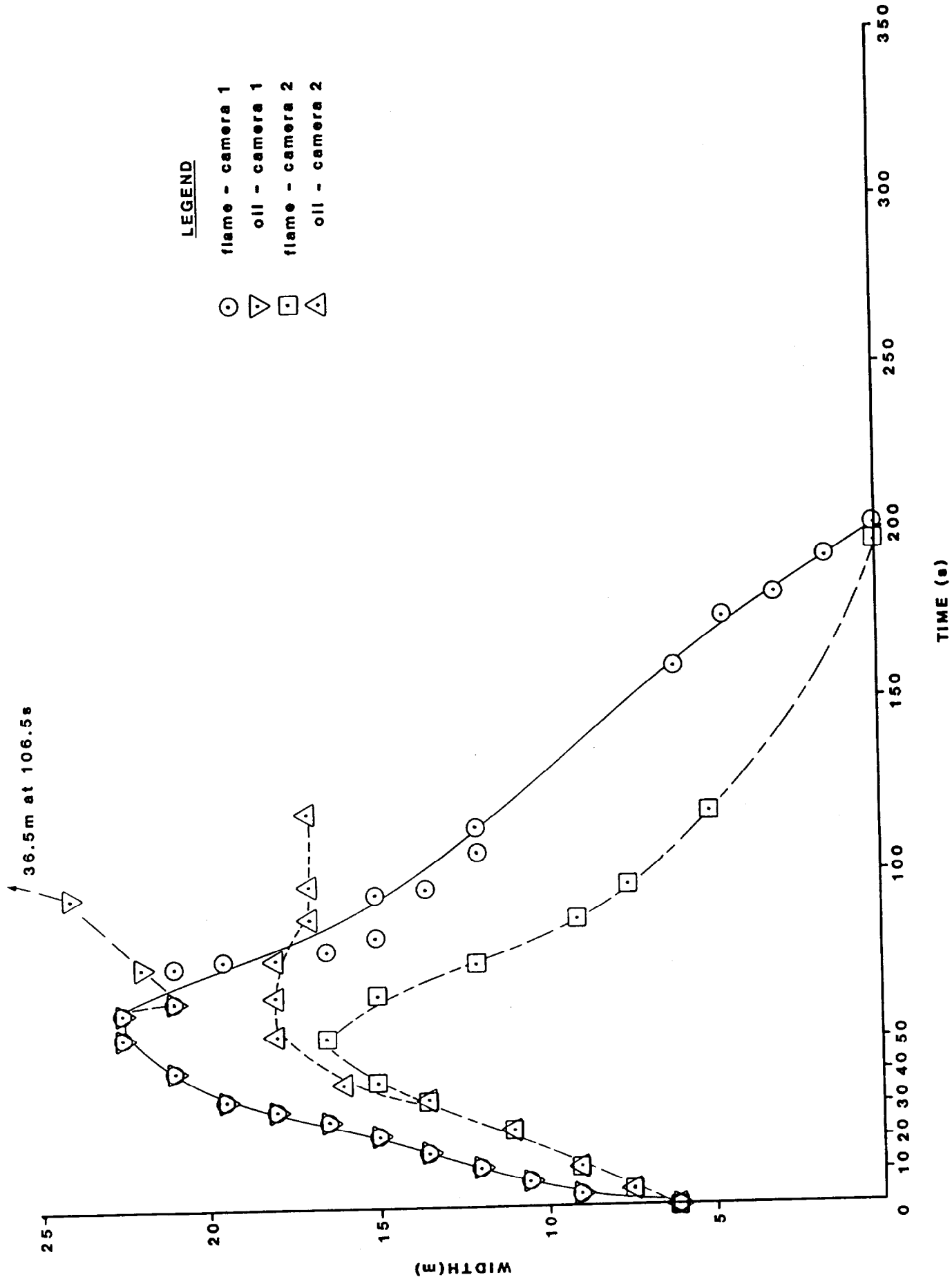

FIGURE 5 CALCULATED OIL AND FLAME AREA - RUN 2

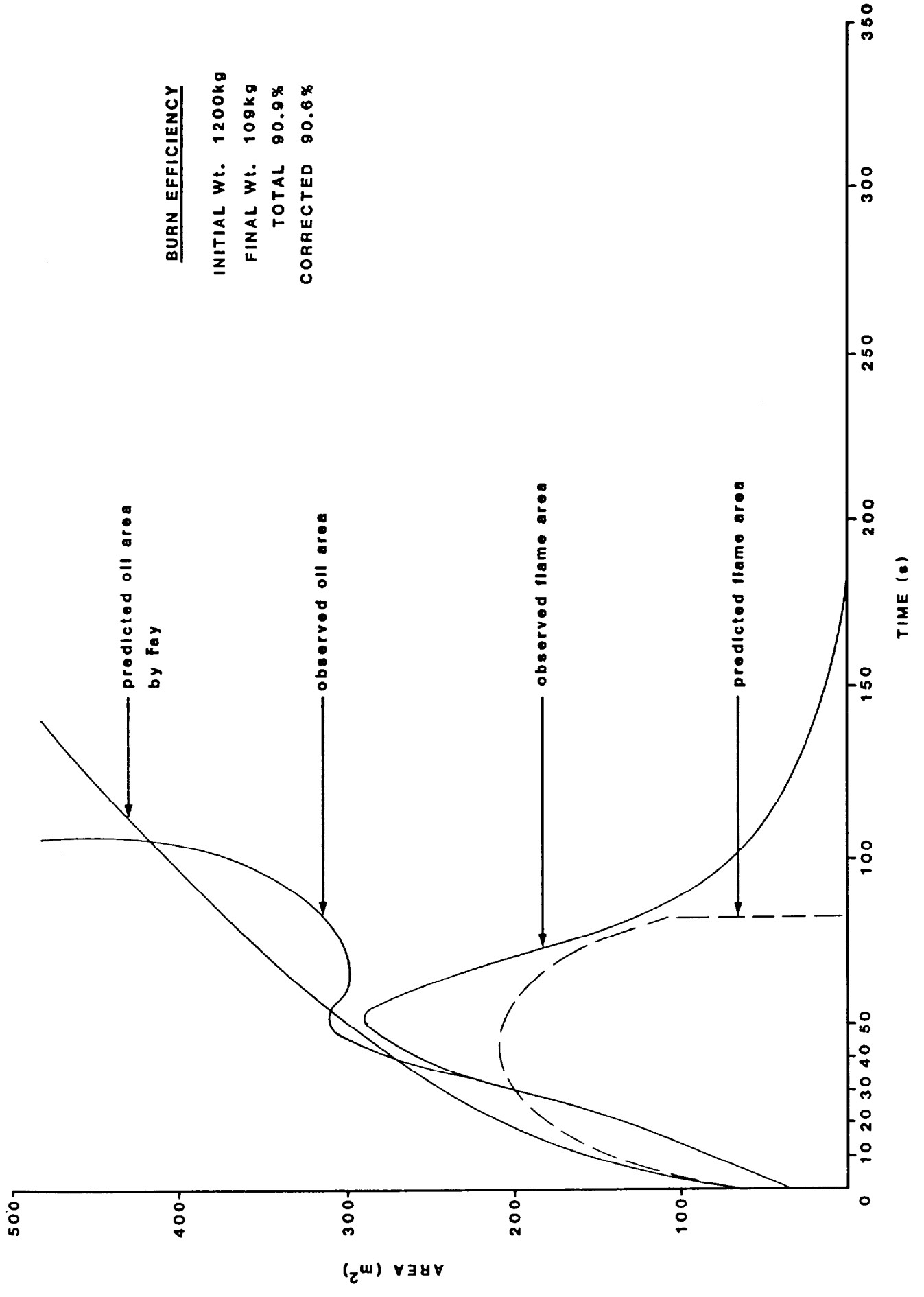

FIGURE 6 FLAME WIDTH - RUN 4

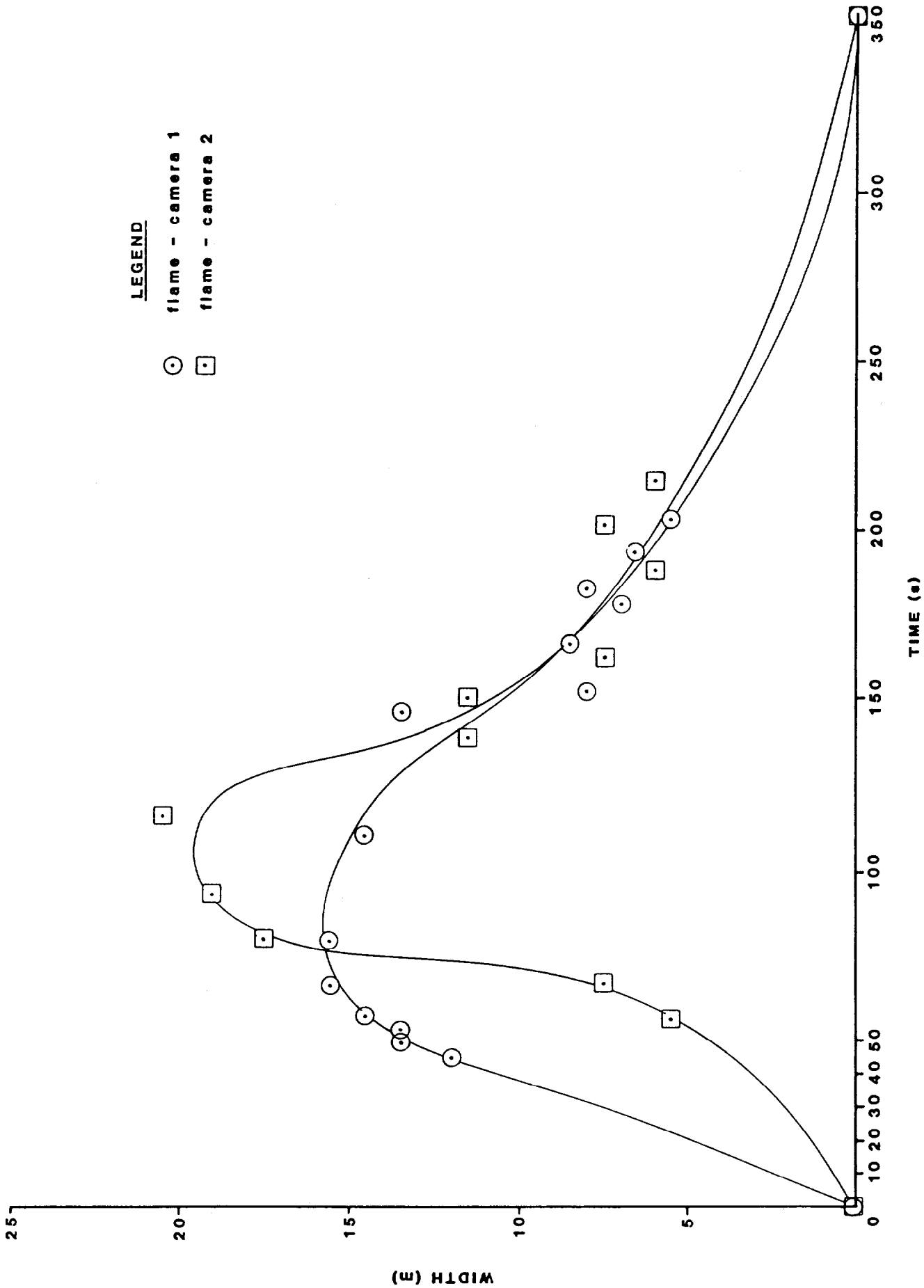

FIGURE 7 CALCULATED FLAME AREA - RUN 4

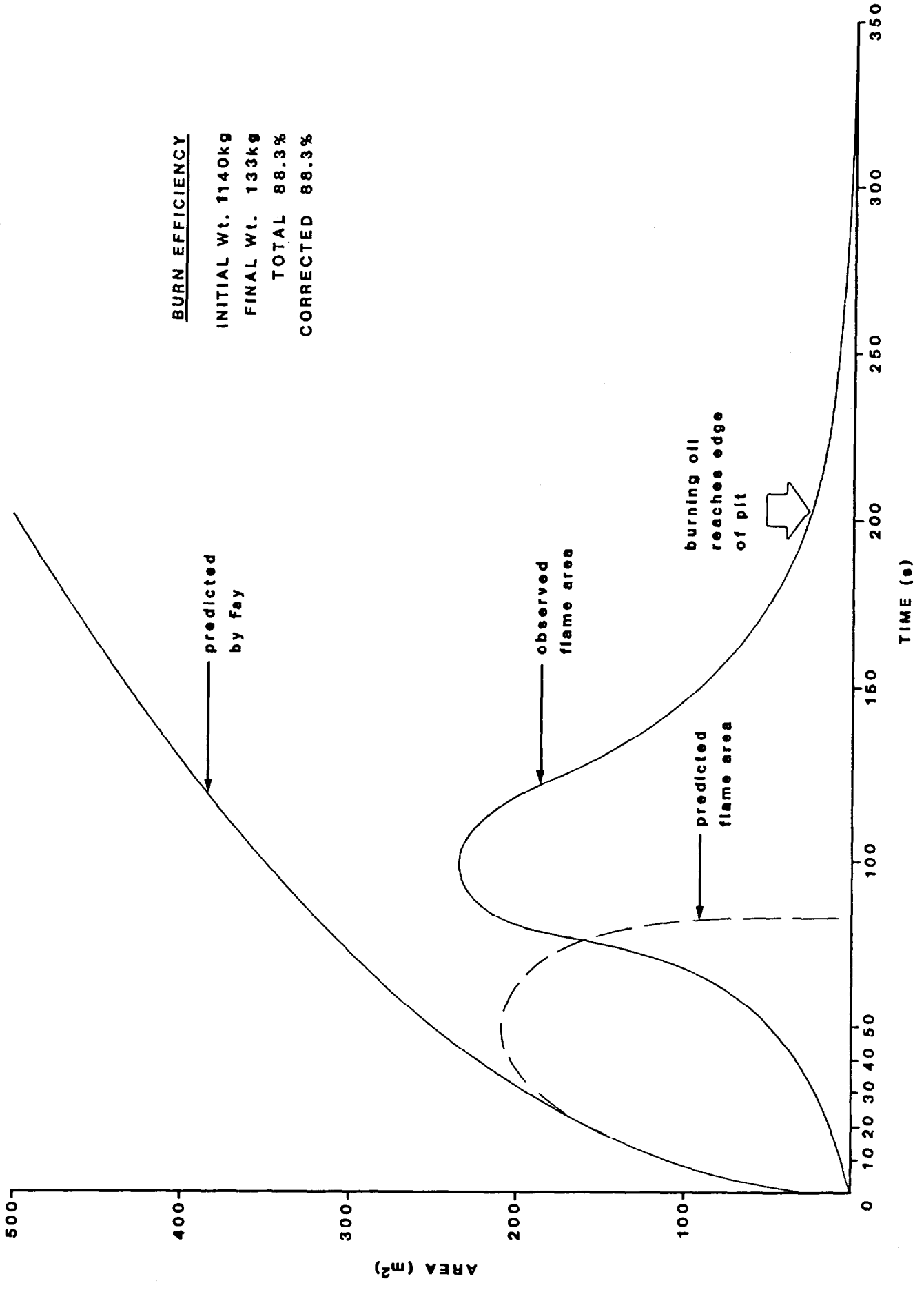

FIGURE 8 AIRFLOW MEASUREMENTS - RUN 3

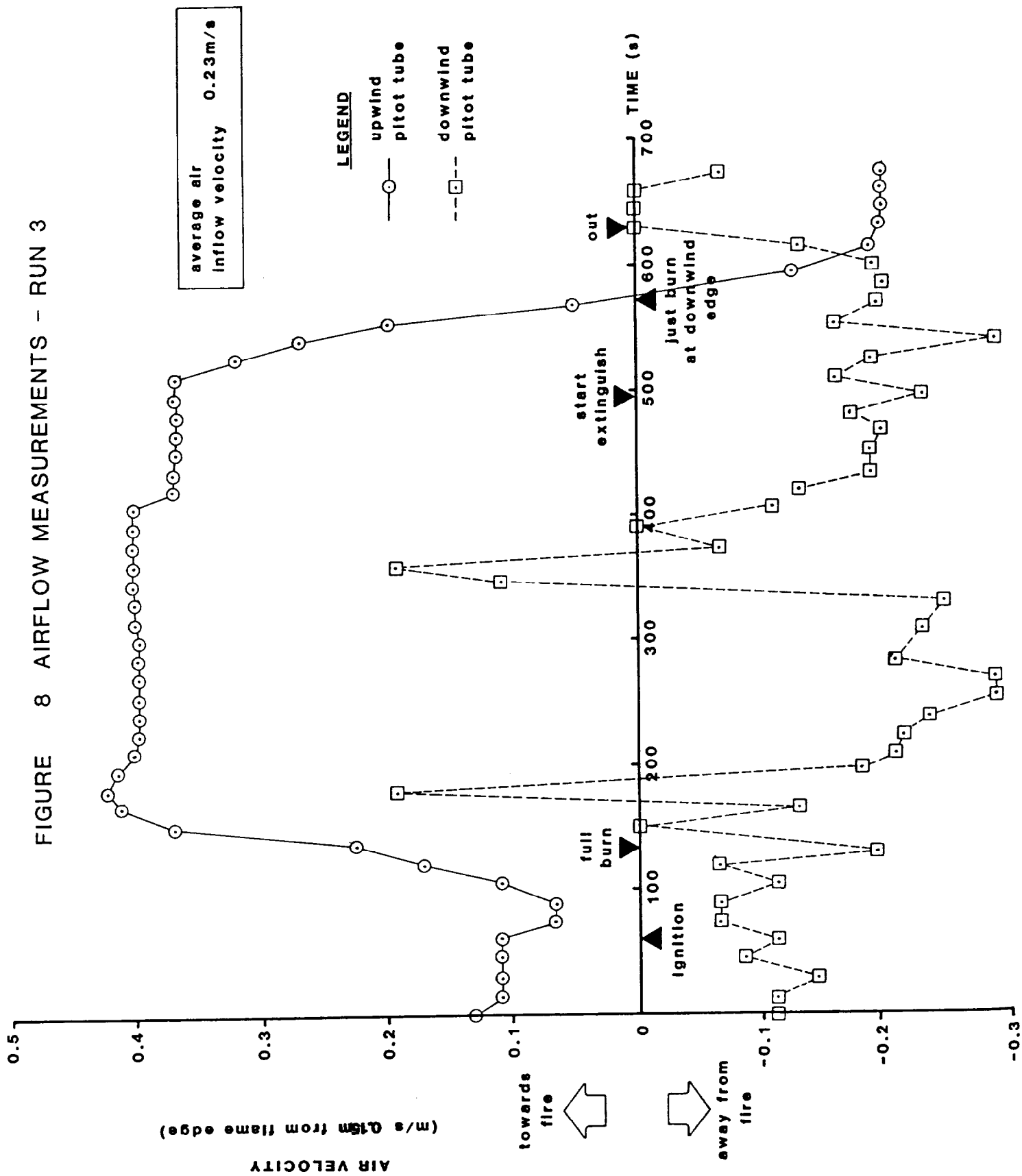

Air Entrainment and Self-Induced Wind-Herding. Figure 8 shows the results of the airflow measurements, upwind and downwind of the fire in test 3. The upwind pitot tube measured a definite induced airflow, with a velocity of about 30 cm/s greater than the ambient wind. The difference in ambient wind speed measured before and after the test may be a result of the light variable winds at the time of the test combined with zero-drift in the electronic manometer and/or chart recorder.

The downwind pitot tube recorded highly turbulent airflows. This fact was confirmed visually by the presence of "dust-devils" downwind of the fire. In fact the downwind pitot tube may have been immersed in flame for much of the burn and the apparent increase in downwind velocity by about 10-15 cm/s may be a component of the buoyant rise velocity of the diffusion flame being bent over by the wind.

The average of the upwind and downwind measurements is a net inflow of air at about 23 cm/s. This agrees with the data of Thomas et al, 1965 for air entrainment into gas burners (about 17 cm/s, 0.25 m above the base of the flame) and with the theory of McCaffrey, 1983 which predicts velocities of 20-25 cm/s at the same height and radius.

In order to model the effects of self-induced wind-herding of a burning oil slick the spreading force of the slick (assumed to be gravity for the slicks of interest) is balanced by the drag on the slick of the radially inward surface current induced by the entrained airflow, ie.:

Gravity force per unit volume = drag force per unit volume, or

$$\Delta\rho g h / \pi^{1/2} r = C_D \rho_A A U^2 / V \qquad (2)$$

where $\Delta\rho$ = density difference between oil and water (kg/m^3)
g = acceleration due to gravity (9.81 m/s^2)
h = slick thickness (m)
r = slick radius (m)
C_D = drag coefficient
ρ_A = density of air (1.28 kg/m^3)
A = area of slick (m^2)
U = air velocity (m/s)
V = oil volume (m^3)

substituting $V = Ah$, and rearranging equation 2 yields

$$h = (\pi^{1/2} C_D \rho_A / \Delta\rho g)^{1/2} U r^{1/2} \qquad (3)$$

It can be shown that, for large fires, U is a constant equal to about 0.25 m/s, in good agreement with the data from test 3. Thus, substituting the value for C_D from the wind tunnel tests (3.5×10^{-3} - S.L. Ross and Energetex, 1985) and = 105 kg/m^3 yields:

$$h = 7 \times 10^{-4} r^{1/2} \qquad (4)$$

This equation predicts a self-induced wind-herded slick thickness of 2.2 mm for a 10 m radius (300 m^2 area) slick, which agrees well with the data for test 2 (see Figure 6.5) which indicates a cessation of oil spreading at 300 m^2 with an estimated thickness (including oil losses to combustion) of 3 mm.

Combustion Efficiency. Figure 9 shows the combustion efficiency as a function of oil volume for both the large scale and mid-scale testing as well as the model predictions. In general, as oil volume increases so does combustion efficiency. Comparison of the large scale data points indicates that:

- instantaneous ignition of the entire slick area results in a higher combustion efficiency than delayed ignition of the periphery (90.6% vs 88.3%).

- ignition of the entire surface area or of the full circumference of the spreading oil is more efficient than ignition of a portion of the downwind slick.

This last point is important for oil spill burning operations. It seems that, unlike burning oil contained in a melt pool, oil is not fed into the area on fire by the wind. In the case of test 1 about 25% of the upwind area of the slick in the containment ring was not on fire upon its release; the burn efficiency for test 1 was about 75% of that of test 2 when the entire slick area was on fire upon release. It seems that a thick, free floating slick, in the absence of large scale eddies, is advected en masse by the wind driven surface currents and unignited oil is not pushed into the fire-zone. Since the upwind flame spreading rates are low (1-2 cm/s) it is unlikely that oil, upwind of a floating ignition source drifting with the slick, would be ignited. Thus it is important to ignite the upwind extremities of a thick slick with conventional igniters or develop an igniter that drifts more slowly than the oil and ignites a long strip of oil from the middle out to the upwind edge.

MODELLING THE BURNING OF UNCONFINED OIL SLICKS

Introduction

The spilled oil is assumed to spread according to the well known laws formulated by Fay: initially a gravity-inertial spread with slick radius proportional to $t^{1/2}$, followed by a gravity-viscous spread with slick radius proportional to $t^{1/4}$. The subsequent surface tension viscous spread is not dealt with because the transition to that regime is uncertain and may occur when the slick is too thin to burn.

It is assumed that the combustion process affects the spread of the slick in only one way, namely that the air flowing into the flame induces a water surface current which opposes the spreading of the slick. This is the self-generated "wind-herding" phenomenon.

The slick continues to burn until its thickness reaches some minimum value at which point the heat loss to the water under the slick uses up all the heat feedback to the slick from the flame above it. The experimental value for this minimum thickness is 0.8mm. The combustion efficiency of the slick is the difference between the volume of the oil spilled and the volume of the remaining layer of unburned residue which has that thickness, divided by the volume of oil spilled. For any given spill volume, the combustion efficiency is maximum when the slick is ignited immediately. Delaying the ignition decreases the efficiency. If ignition is delayed until the slick thickness is less than 0.8mm, none of the oil can burn, and the combustion efficiency is zero.

FIGURE 9 COMBUSTION EFFICIENCY - INSTANTANEOUS IGNITION

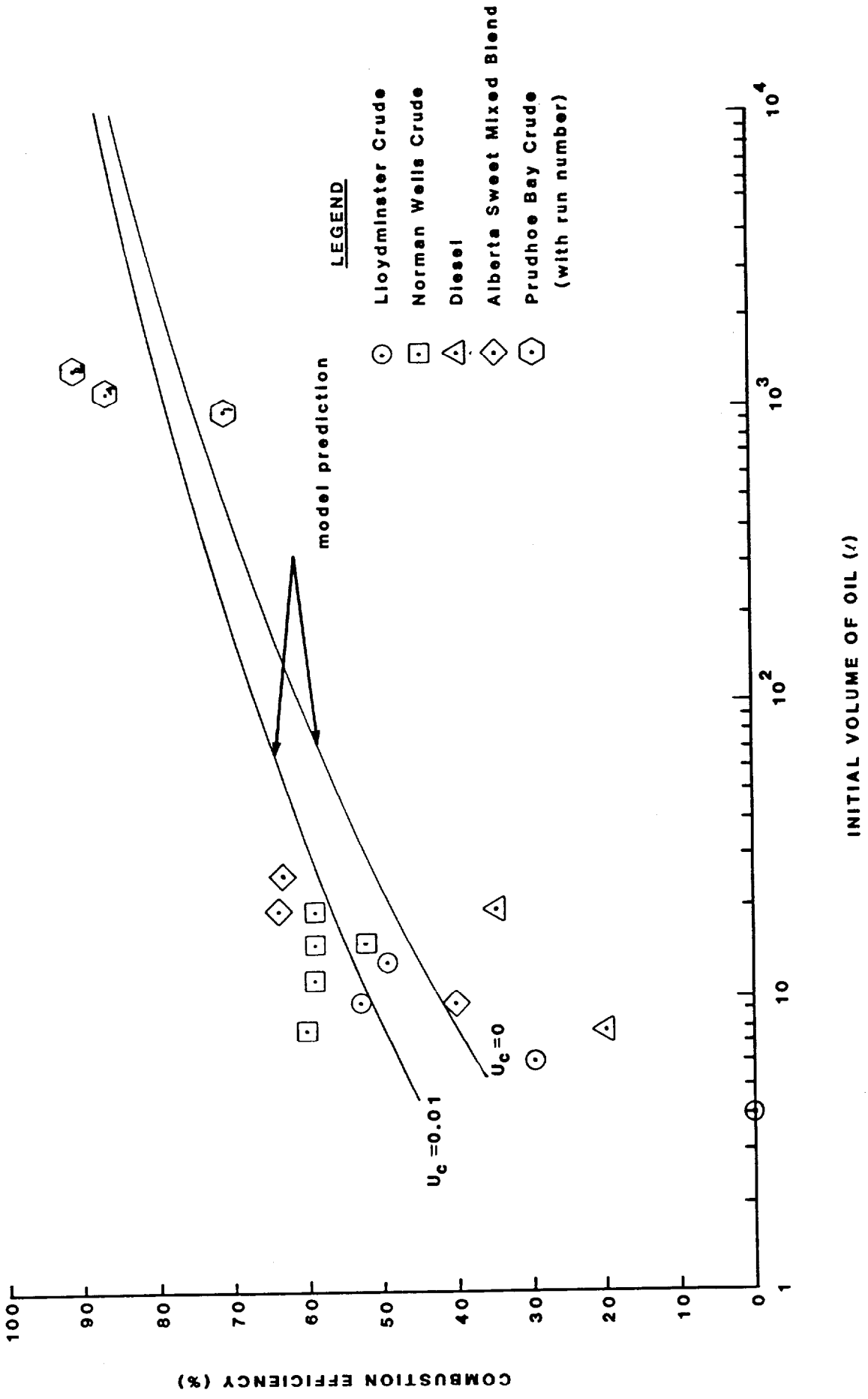

The equations of the spreading burning slick were solved for four spill volumes: 0.01, 1.0, 10^2 and 10^4 m^3. The calculations were performed with two values of the induced water current: zero and 0.01 m/s, over a wide range of ignition delay times. Details of the model may be found in the project report (S.L. Ross and Energetex 1985).

Results

Combustion Efficiency for Immediate Ignition. The computed values of combustion efficiency, η_{comb} as well as the burning time, t_b and the radius of the slick at extinction, $r_{s,q}$ are listed in Table 3. The results are shown for two values of induced water surface current: 0 and 0.01 m/s.

TABLE 3

COMBUSTION EFFICIENCY, BURNING TIME AND RADIUS OF SLICK AT EXTINCTION

V_s, m^3	u_c,(m/s)	t_{burn},(s)	$r_{s,q}$,(m)	η_{comb}(%)
10^{-2}	0	19.9	1.48	44.3
	0.01	25.9	1.35	54.0
1	0	80.7	9.78	76.2
	0.01	88.5	9.20	78.9
10^2	0	270	61.2	91.2
	0.01	277	58.8	91.2
10^4	0	860	375	95.8
	0.01	876	369	96.5

The effect of the induced current is to increase the burning time and the combustion efficiency and to decrease the size of the slick when burning ceases. The effect is minor in the case of all but the smallest spill studied. A rough estimate of η_{comb} can be obtained by manipulating equation 4 to yield:

$$\eta_{comb} = (1 - 1/3 V_s^{1/5}) \times 100\% \qquad (5)$$

Calculations were also attempted with a higher value of the induced surface current, u_c = 0.1 m/s. Solutions could be obtained only for the two largest spills with that value. The trend shown in Table 3 continued in both cases.

Combustion Efficiency with Ignition Delay. The computed values for combustion efficiency are plotted in Fig. 10 as a function of the ignition delay $_d$. Four pairs of curves are shown, one pair for each of the following values of V_s: 10^{-2}, 1, 10^2 and 10^4 m^3.

One curve in each pair was calculated for zero surface current ($u_c = 0$). The other was calculated for $u_c = 0.01$ m/s. In each case the combustion efficiency decreases from a maximum value at the smallest delay. The values shown for $\tau_d = 10$ are for all intents and purposes the same as those for zero delay.

In the case of zero surface current, the curves of η_{comb} approach zero continuously. With $u_c = 0.01$ m/s, the curves were very similar to those for $u_c = 0$ but only up to a point. At a certain value of τ_d, the equations could no longer be solved. The slick thickness began to increase, the slick radius decreased, and the burning rate began to decrease drastically. This behaviour occurred for all higher values of τ_d.

It is very likely that the actual value of u_c lies somewhere between 0 and 0.01 m/s (assuming the surface water moves at 3% of the wind speed the value of u_c measured during the large scale trials is 0.23 x 0.03 = 0.007m/s). This means that in practice one could expect at least a rapid decrease of n with delay time beyond the threshold value.

The threshold value of $_d$ is identified as the maximum possible delay in igniting the slick. If ignition is delayed any longer, burning may be ineffective. The values of the maximum ignition delay are listed in Table 4. Also included are x_q (the dimensionless radius at extinction) and η_{comb} for the maximum delay.

TABLE 4

MAXIMUM IGNITION DELAY $_{d,max}$

AND CORRESPONDING $_{q}$, x_q AND η_{comb}

V_s,(m^3)	$\tau_{d,max}$,(s)	τ_q	at $\tau_{d,max}$ x_q	η_{comb},(%)
10^{-2}	125	190	8.322	19.3
1	500	665	14.127	49.8
10^2	1,950	2,312	24.392	68.0
10^4	7,150	7,830	41.555	79.8

The maximum permissible ignition delay can be correlated with spill size. An excellent correlation is obtained in the form of a power law. In dimensional form it can be expressed as

$$t_{d,max} = 0.0975 V_s^{0.46} \qquad (6)$$

where $t_{d,max}$ = maximum permissable delay time between the occurence of the spill and its ignition; (hours)

V_s = spill volume;(m^3).

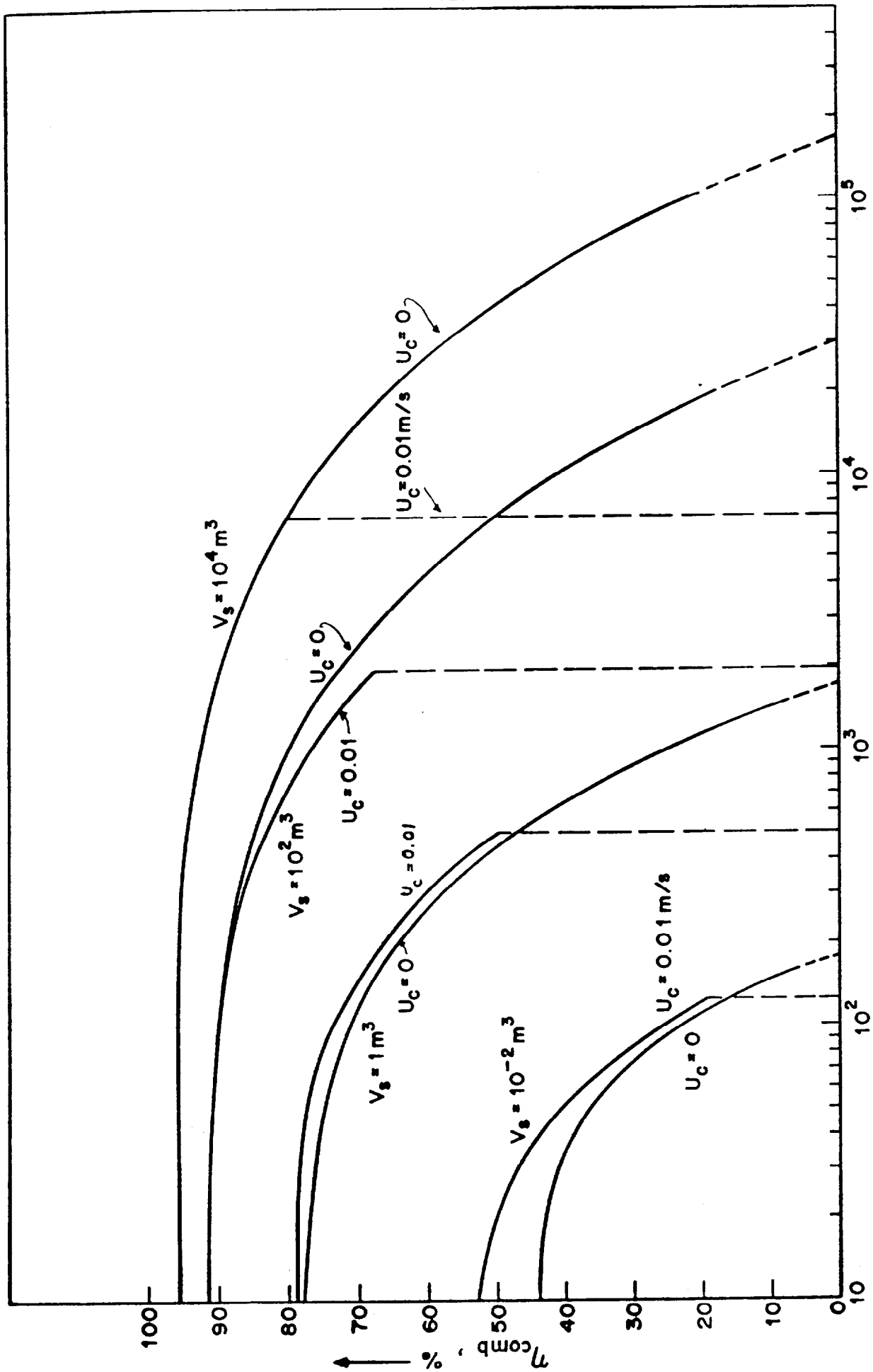

FIGURE 10 — COMBUSTION EFFICIENCY AS A FUNCTION OF IGNITION DELAY

Equation (6) is plotted in Figure 11.

A rough but useful approximation to equation (6) is

$$t_{d,max} = 0.1\ V_S^{1/2} \qquad (7)$$

which quickly gives the order of magnitude of the maximum delay.

The delayed ignition of a spreading slick is accomplished by placing igniters around its perimeter. The flame spreads outwards with the burning oil. Its inward spread is aided by the inward wind induced by the flames at the periphery.

Igniters should be placed 3 m apart around the perimeter of the slick. The slick radius at $t_{d,\,max}$ is one of the results of the calculations. Therefore, the number of igniters needed to achieve ignition with the maximum permissible delay can be calculated. The results are presented in Table 5.

TABLE 5

NUMBER OF IGNITERS NEEDED AT THE MAXIMUM IGNITION DELAY

$V_S, (m^3)$	Number Needed
10^{-2}	4
1	30
10^2	238
10^4	1,875

These results are also well correlated by a power law.

$$N = 31\ V_S^{0.45} \qquad (8)$$

Equation (8) is also shown in Figure 11. The difference between the power of V_S in equations (7) and (8) cannot be significant. On that basis, the number of igniters needed to burn the slick after the maximum delay is proportional to that delay. The proportionality is about 320 igniters per hour. However to avoid confusion and keep the dependence on spill size in mind, it is preferable to use Fig. 11 to calculate both the maximum permissible delay and the number of igniters then required.

Additional results are presented in the report. They include the scaling factors for time and slick radius, as well as the parameters of the slicks whose behaviour was calculated.

CONCLUSIONS

* The ignition and burning of uncontained batch oil spills seems to be a feasible countermeasure for certain open water spills.

* Combustion efficiency is primarily a function of spill volume; the larger the spill the higher the combustion efficiency (in excess of 90% for spills greater than 1 m^3 ignited instantaneously). A rough approximation of the combustion efficiency for an instantaneously ignited slick is:

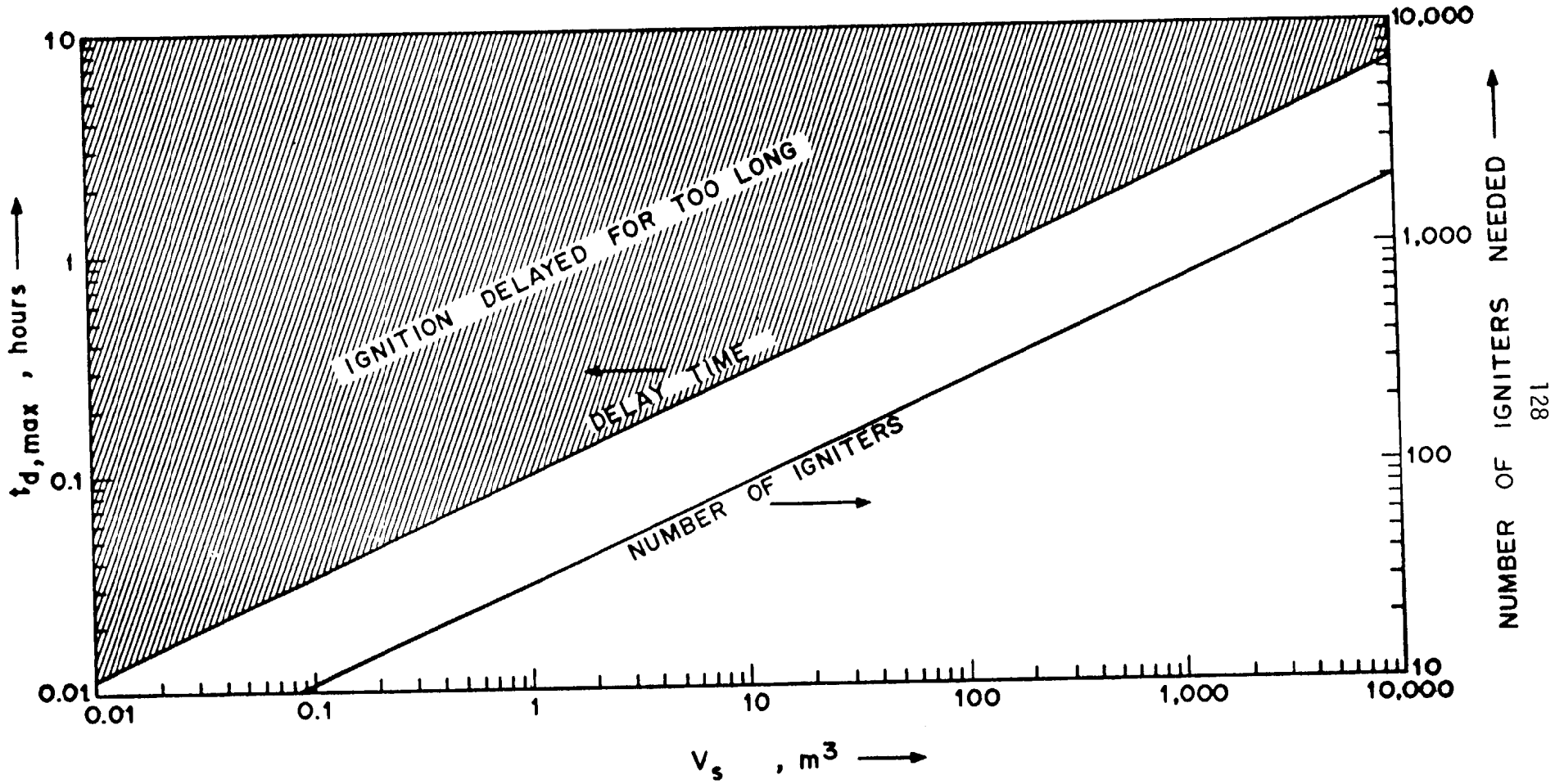

FIGURE 11 — MAXIMUM PERMISSIBLE IGNITION DELAY TIME AND THE NUMBER OF IGNITERS REQUIRED AT THAT TIME AS A FUNCTION OF SPILL VOLUME

$\eta_{comb} = (1 - 1/3 V_s^{-1/5}) \times 100\%$ V_s in m^3

* The sooner a slick is ignited the higher the combustion efficiency. The maximum permissible ignition delay can be estimated by:

  $t_{d, max} = 0.1\ V_s^{1/2}$ $t_{d, max}$ in hours, V_s in m^3.

* Ignition of the periphery of the slick results in almost as high combustion efficiencies as ignition of the entire surface area. The required number of conventional igniters at the miximum ignition delay can be estimated by:

  $N = 31\ V_s^{0.45}$ V_s in m^3

* Air, entrained by the combustion of the oil slick at a velocity of about 0.25 m/s, induces an inward surface current which inhibits and finally stops the oil's spread. The slick thickness at which this occurs is related to the size of the fire and can be estimated by:

  $h = 7 \times 10^{-4} r^{1/2}$ h and r in m

RECOMMENDATIONS

* Field trials involving larger oil volumes (10 to 100 m^3) are required to:

  - assess the effect of longer ignition delay times than are possible with smaller spills.
  - determine the effects of waves and ocean turbulence on the burning, and
  - further calibrate the mathematical models.

* The use of spills of opportunity should also be considered to assess the above effects.

* A technique should be developed for effectively deploying commercially-available igniters around a slick; also the development should be undertaken of a new igniter that moves relatively from the centre to the periphery of a slick.

REFERENCES

Buist, I.A. and E.M. Twardus. 1984. In-Situ Combustion of Uncontained Oil Slicks. Proceedings of the Seventh Annual Arctic Marine Oilspill Program Technical Seminar, Edmonton. pp. 127-154.

Fay, J.A. 1969. The Spread of Oil Slicks on a Calm Sea. Massachusetts Institute of Technology. Boston.

McCaffrey, B.J. 1976. A Robust Bidirectional Low-Velocity Probe for Flame and Fire Application. Combustion and Flame. 25. pp. 125-127

McCaffrey, B.J. 1983. Momentum Implications for Buoyant Diffusion Flames. Combustion and Flame. 52. pp. 149-167

S.L. Ross Environmental Research Limited and Energetex Engineering. 1985. In-Situ Burning of Uncontained Oil Slicks. Draft report to Environment Canada. Ottawa.